An analysis of inhibitory junction potentials in the guinea-pig proximal colon

G. D. S. Hirst[1], R. A. R. Bywater[2], N. Teramoto[3] and F. R. Edwards[1]

[1]*Division of Neuroscience, John Curtin School of Medical Research, Australian National University, Canberra, ACT, Australia*
[2]*Department of Physiology, Monash University, Clayton, Victoria, Australia*
[3]*Department of Pharmacology, Graduate School of Medical Sciences, Kyushu University, Fukuoka, 812-8582, Japan*

Intracellular recordings were made from either sheets or isolated bundles of the circular muscle layer of guinea-pig proximal colon and the responses evoked by stimulating inhibitory nerve fibres were analysed. Inhibitory junction potentials (IJPs), evoked by single stimuli, had two components which could be separated on their pharmacological and temporal characteristics and their voltage sensitivities. The initial component, which was abolished by apamin and reduced in amplitude by pyridoxalphosphate-6-azophenyl-2′,4′-disulphonic acid (PPADS), had a brief time course: its amplitude was changed when the external concentration of potassium ions ($[K^+]_o$) was changed. The second component of the IJP had a slower onset than the first component, was abolished by L-nitroarginine (NOLA) and oxadiazolo quinoxalin-1-one (ODQ), an inhibitor of soluble guanylate cyclase: its amplitude was little affected by changing $[K^+]_o$ and was increased when the membrane potential of the circular layer was hyperpolarized. The observations suggest that the initial component of the IJP results from the release of ATP which triggers an increase in membrane conductance to K^+ and that the second component results from the release of nitric oxide which suppresses a background inward current.

(Received 21 March 2004; accepted after revision 11 June 2004; first published online 11 June 2004)
Corresponding author G. D. S. Hirst: Division of Neuroscience, John Curtin School of Medical Research, Australian National University, Canberra, ACT, Australia. Email: david.hirst@anu.edu.au

The activity of gastrointestinal smooth muscle reflects a balance between myogenic, neural and hormonal factors. Recently it has been shown that interstitial cells of Cajal (ICC) are involved in normal patterns of myogenic activity and in the neural pathway by which excitatory and inhibitory nerve terminals modify gut motility. In the gastric antrum, slow waves are initiated by a network of ICC lying in the myenteric region (ICC_{MY}) and the attenuated waves of depolarization are augmented by a secondary wave of depolarization generated by a set of intramuscular ICC distributed amongst the muscle layers (ICC_{IM}; Hirst & Ward, 2003). In the antrum the secondary wave of depolarization generated can be initiated in single bundles of circular muscle which lack ICC_{MY} but which contain ICC_{IM}, simply by depolarizing the bundle, indicating that the activity of antral ICC_{IM} is influenced by membrane potential (Suzuki & Hirst, 1999; Edwards *et al.* 1999; Van Helden *et al.* 2000; Fukuta *et al.* 2002; Kito *et al.* 2002). However, not all gastric ICC_{IM} demonstrate such voltage sensitivity, with those in the fundus being little affected by changes in membrane potential (Beckett *et al.* 2004).

In the stomach, ICC_{IM} also form an essential part of the pathway by which neuronal information is transferred to smooth muscle cells, with the responses to either inhibitory or excitatory nerve stimulation being greatly attenuated in murine gastric antral and fundal tissues devoid of ICC_{IM} (Burns *et al.* 1996; Ward *et al.* 2000; Beckett *et al.* 2002; Suzuki *et al.* 2003; Hirst & Ward, 2003). When membrane potential recordings were made from bundles of circular muscle isolated from either the antrum or fundus, the recordings were dominated by discharges of membrane noise but only if ICC_{IM} were present (Dickens *et al.* 2001; Beckett *et al.* 2002, 2004). The membrane noise results from a discharge of spontaneous depolarizing potentials, termed unitary potentials (Edwards *et al.* 1999). In the gastric antrum unitary potentials result from Ca^{2+} release from IP_3-dependent intracellular Ca^{2+} stores (Suzuki & Hirst, 1999; van Helden *et al.* 2000; Suzuki *et al.* 2000), followed by the activation of anion-selective channels

 DOI: 10.1113/jphysiol.2004.065052

(Hirst *et al.* 2002*b*). In the fundus unitary potentials appear to have a similar origin but the channels activated by each increase in the internal concentration of calcium ions ($[Ca^{2+}]_i$) differ from those in the antrum in that they are not blocked by blockers of anion selective channels (Beckett *et al.* 2004). In many regions of the gut, inhibitory nerve stimulation evokes a biphasic inhibitory junction potential, IJP, consisting of an apamin-sensitive fast IJP which is followed by longer-lasting, apamin-insensitive nitrergic IJP (Niel *et al.* 1983*a*; Dalziel *et al.* 1991; Lyster *et al.* 1992; He & Goyal, 1993; Zhang & Patterson, 2002; Suzuki *et al.* 2003). In the antrum analyses of the nitrergic component show that it results from a suppression of the resting discharge of unitary potentials by ICC_{IM}, with neurally released nitric oxide (NO) causing the formation of cyclic GMP (Suzuki *et al.* 2003; Teramoto & Hirst, 2003). Similarly, analyses of antral cholinergic excitatory junction potentials indicate that they result from an increased rate of discharge of unitary potentials by ICC_{IM} (Hirst *et al.* 2002*c*).

The present experiments were carried out with the aim of analysing the properties of IJPs recorded from the proximal colon. In this tissue inhibitory nerves preferentially innervate ICC_{IM} (Wang *et al.* 2000) but the functional correlate of these structural findings is not known. The experiments reported here have reconfirmed the biphasic nature of colonic IJPs and have examined the properties of the two separate components. The results are discussed in relation to the idea that the initial component results from an increase in potassium conductance (g_K) whereas the secondary nitrergic component of the IJP results from a suppression of the discharge of unitary potentials by colonic ICC_{IM}.

Methods

Preparations and recording techniques

The procedures described were approved by the Animal Experimentation Ethics Committee at the Australian National University. Guinea-pigs of either sex, weight range 250–400 g, were stunned, exsanguinated and the proximal colon removed. The proximal colon was opened along its mesenteric border. Segments of colon were pinned out in a dissecting chamber filled with oxygenated physiological saline (composition, mM): NaCl, 120; $NaHCO_3$, 25; NaH_2PO_4, 1.0; KCl, 5; $MgCl_2$, 2; $CaCl_2$, 2.5; and glucose, 11; bubbled with 95% O_2–5% CO_2. After removing the mucosa and the longitudinal muscle layer, two distinct types of preparation were made. For some experiments, sheets of tissue, approximately 5 mm square were dissected free and pinned in a recording chamber, mucosal surface downwards. For other experiments thin strips of circular muscle (diameter 80–150 μm, length 400–600 μm) were isolated as previously described (Suzuki & Hirst, 1999) and pinned in a recording chamber. These strips of tissue contained some three to five individual bundles of smooth muscle. However when recordings were made from adjacent bundles in the same strip, they appeared to be electrically isolated from each other. Thus the discharge patterns of membrane noise were different and current injected into one bundle failed to produce an electrotonic potential in the second bundle. With either preparation, intramuscular nerve terminals were stimulated using a pair of platinum stimulating electrodes, positioned one on either side of the preparation (Hirst *et al.* 2002*c*). The sheet preparations were impaled with single sharp microelectrodes (resistance 90–150 MΩ, filled with 0.5 M KCl). Individual bundles of muscle were impaled with two independently mounted sharp electrodes; one was used to record membrane potential changes and the other to inject current. Membrane potential changes and membrane currents were amplified using an Axoclamp-2B amplifier (Axon Instruments, Foster City, CA, USA), low pass filtered (cut-off frequency, 100 Hz) digitized and stored on computer for later analysis. During each experiment the preparation was constantly superfused with physiological saline solution warmed to 37°C; nifedipine (1 μM) was added to the physiological saline to reduce muscle contractility: atropine (1 μM) was also added to abolish the effects of stimulating excitatory cholinergic nerves. In several experiments spectral density curves were constructed from membrane potential recordings obtained from the isolated bundles of colonic muscle (see Edwards *et al.* 1999). In other experiments, the standard deviation time course was determined for baseline recordings and during the nitrergic IJP (Baylor & Hodgkin, 1973; Edwards *et al.* 1976). All data are expressed as means ± standard error of the means (S.E.M.). Student's *t* tests were used to determine if data sets differed, *P* values of less than 0.05 were taken to indicate significant differences between sets of observations.

Simulations of IJPs

A segment of a single bundle of circular muscle was assumed to be electrically isopotential so that its electrical behaviour could be modelled by a single equivalent cell. In the first instance, resting membrane conductances were represented as ohmic leaks of K^+ (g_K), Cl^- (g_{Cl}) and Na^+

(g_{Na}) with equilibrium potentials of −90, −20 and 40 mV, respectively (Fig. 1*A*). Absolute values of g_K (98 nS), g_{Cl} (73 nS) and g_{Na} (30 nS) were chosen to give a resting membrane potential of −45 mV (see Results) and an input resistance of 5 MΩ. Membrane capacitance (C_m) was set to 30 nF which gave a membrane time constant of 150 ms, close to the mean value for circular smooth muscle bundles, determined experimentally. The early purinergic component of the IJP was modelled as a transient increase in g_K (Fig. 5*B* and *C*). The time course of the modulation was defined as the difference between two exponential functions, raised to a power, *N*:

$$g = M(\exp(-t/A) - \exp(-t/B)^N \quad \text{for } t > 0 \qquad (1)$$

where *g* represented the modulation in g_K, *M* scaled the peak modulation to 14 nS, *A* and *B* took values of 0.2 s and 0.1 s, respectively, and the exponent *N* was 1. In the first instance the nitrergic component of the IJP was modelled as an additional slower more sustained increase in g_K (Fig. 5*B*), using eqn (1) with the value for *M* chosen to give a peak increase of 100 nS, with *A* and *B* taking values of 0.9 s and 0.85 s and *N* taking a value of 1.6. In the subsequent simulation the late component of the IJP was modelled as a transient reduction in g_{Na} (Fig. 5*C*). Using eqn (1), *M* was chosen to give a 98% peak reduction in g_{Na}, with *A* and *B* taking values of 1 s and 0.95 s, respectively, and *N* taking a value of 2. The equation which describes the time course of the membrane potential (E_m) of the equivalent cell is:

$$dE_m/dt = \Sigma I_{ionic} + I_{electrode} \qquad (2)$$

where ΣI_{ionic} is the sum of resting membrane currents and transient membrane currents resulting from imposed transient membrane conductance modulations. $I_{electrode}$ represents current injected into the bundle via a microelectrode. No attempt was made to simulate the rebound depolarization that was evident in recordings of IJPs.

A second model (Fig. 1*B*) was proposed for the membrane that contained an additional membrane conductance under baseline conditions. Previously the all resting membrane conductances were time invariant. In the second model the additional conductance was proposed to be dependent on an ongoing discharge of unitary conductance modulations. It was therefore a time-varying conductance, $g_{cation}(t)$, under baseline conditions. In guinea-pig antral tissue, unitary conductance changes occur at Poisson distributed intervals, and have characteristic skewed amplitude distributions (Edwards *et al.* 1999). Again, eqn (1) provides a description of their average individual time course in proximal colon with *A* set to 0.525 s, *B* set to 0.035 s and *N* set to 3. The amplitude distribution employed was that observed in antral tissue (Edwards *et al.* 1999), but with a reduced mean value to approximate those seen in proximal colon. The equilibrium potential for unitary conductance events was estimated to be +12.5 mV (see Results). The inclusion of $g_{cation}(t)$ required adjustments to the values of the existing resting membrane conductances in order to maintain the input resistance of the equivalent cell at 5 MΩ, and the resting membrane potential at −45 mV. Accordingly, the resting membrane conductances were made 94 nS (g_K), 56 nS (g_{Cl}) and 5 nS (g_{Na}). Ratios between these conductance values were in approximate concordance with the permeability coefficients cited by

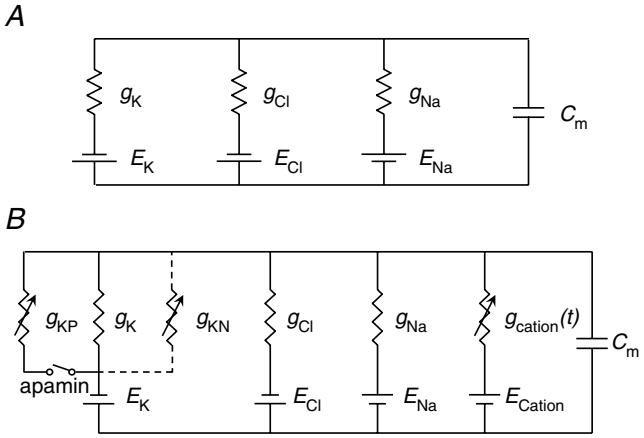

Figure 1. Equivalent electrical circuits used to simulate the time courses of IJPs recorded from the circular layer of the proximal colon

A illustrates the simple electrical circuit used to simulate the time courses of IJPs recorded the distal colon. The early purinergic component of the IJP was modelled as a transient increase in g_K whose time course of the modulation was defined as the difference between two exponential functions, raised to a power, *N* (eqn (1)). The nitrergic component of the IJP was modelled as an additional slower more sustained increase in g_K again using eqn (1). The time course of the membrane potential change (E_m) of the equivalent cell is given by eqn (2). No attempt was made to simulate the rebound depolarization that was evident in recordings of IJPs. *B* illustrates the electrical circuit used to simulate the time courses of IJPs when a tonic depolarization was assumed to be generated by ICC_{IM}. This additional conductance was proposed to be dependent on an ongoing discharge of unitary conductance modulations. The purinergic K^+ conductance (g_{KP}) proposed in the first model (*A*) was made explicit in *B* and is shown connected via a switch indicating that current via this conductance was reduced to zero in the presence of apamin. Values used for g_{KP} modulation were as in the first model. Similarly the nitrergic K^+ conductance (g_{KN}) proposed in the first model (*A*) is also made explicit in *B* and is shown connected by dashed lines indicating that it is a candidate model for the late phase of the IJP. Values used for g_{KN} modulation were as in the first model. The alternative model of the nitrergic component of the IJP was a transient reduction in the rate of discharge unitary potentials.

Casteels (1969). At a resting discharge rate of 270 Hz, the mean value of $g_{\text{cation}}(t)$ was 42 nS, giving the equivalent cell the required input resistance and resting membrane potential. When $g_{\text{cation}}(t)$ was reduced to zero, the resting membrane potential hyperpolarized to −60 mV. Thus, $g_{\text{cation}}(t)$ contributed some 15 mV to the resting membrane potential.

The purinergic K^+ conductance (g_{KP}) proposed in the first model (Fig. 1*A*) was made explicit in Fig. 1*B* and is shown connected via a switch indicating that current via this conductance was reduced to zero in the presence of apamin. Values used for g_{KP} modulation were as in the first model. Similarly the nitrergic K^+ conductance (g_{KN}) proposed in the first model (Fig. 1*A*) is also made explicit in Fig. 1*B* and is shown connected by dashed lines indicating that it is a candidate model for the late phase of the IJP. Values used for g_{KN} modulation were as in the first model to obtain the simulations shown in Fig. 7*A*. Current injection via a microelectrode was simulated by setting $I_{\text{electrode}}$ in eqn (2) to −3 nA to obtain 15 mV of hyperpolarization and to −6 nA to obtain 30 mV of hyperpolarization.

The alternative model of the nitrergic component of the IJP was a transient reduction in the rate of discharge unitary potentials. Equation (1) was again used to generate this modulation in rate, with the value for *M* chosen to give a reduction from the resting discharge rate of 270 Hz to a discharge rate of zero, and values of 0.701 s for *A*, 0.7 s for *B* and 1 for *N*. The mean membrane conductance due to the discharge of unitary events, $g_{\text{cation}}(t)$, reduced from 42 nS at resting discharge rate to 0 nS at peak modulation. These values yielded the simulations shown in Fig. 7*B*. Figure 8*A* and *B* show simulations analogous to those in Fig. 7*A* and *B*, with the difference that apamin was absent from the preparation. The equivalent circuit is that shown in Fig, 1*B*, but with the switch labelled 'apamin' in the closed state. The purinergic K^+ conductance, g_{KP}, was simulated using the values specified in the first model. The alternative models of the late IJP component, g_{KN} increase or unitary discharge rate decrease, were added, respectively, to the purinergic response and are shown in Fig. 8*A* and *B*. All simulations involving $g_{\text{cation}}(t)$ (Figs 7*A* and *B*, 8*A* and *B*, 9*A–D*) were repeated in cohorts of 40 trials, each with a random sample of unitary discharge from the same statistical generating function, but distinct values of amplitudes and times of occurrence. Mean time courses, and standard deviation time courses, were calculated from each set of 40 trials and these are shown in the figures. Simulations were carried out using Matlab 6.5.1 (The Mathworks, Inc., Natick, MA, USA) running on a Pentium IV computer.

Drugs

L-Nitroarginine (NOLA) and acetoxymethyl ester tris-(2-amino-S-phenoxy) ethane-N,N,N′,N′-tetracetic acid (MAPTA-AM) (obtained from Calbiochem, San Diego, CA, USA), apamin, atropine sulphate, glibenclamide, iberiotoxin (IbTX), nifedipine, niflumic acid (NFA), oxadiazolo quinoxalin-1-one (ODQ), 4,4′-diisothiocyano-2,2′-stilbene disulphonic acid (DIDS), anthracene-9-carboxylic acid (9-AC) (each obtained from Sigma Chemical Co., St Louis, MO, USA) and pyridoxalphosphate-6-azophenyl-2′,4′-disulphonic acid (PPADS, obtained from Research Biochemical International, Natick, MA, USA) were used in these experiments.

Results

General observations

When intracellular recordings were made from sheets of the circular layer of the proximal colon, cells had resting potentials in the range −35 to −52 mV (−44.9 ± 1.0 mV, $n = 44$: mean ± S.E.M., where each n value represents an observation made on a separate preparation). In most preparations the membrane potential recordings displayed an ongoing discharge of membrane noise: in a further nine preparations, which are not included in the report, regular discharges of rhythmical depolarizing potentials with amplitudes of up to 35 mV were detected. The nature of these oscillations has not been investigated further. In the quiescent preparations, when nerve terminals present in the circular layer were stimulated with a single pulse (pulse width 0.02–0.1 ms, intensity 10–70 mA) an IJP was evoked. The amplitude of the IJP could be graded by altering the stimulus strength up to a maximum value: in all experiments the stimulus strength was set some 20% higher than that used to evoke the largest amplitude IJP and left unchanged for the duration of the experiment. In control solutions IJPs, evoked by supramaximal stimuli, had a mean peak amplitude of 22.1 ± 0.9 mV ($n = 44$), a mean latency, defined as the time to 5% of their peak amplitudes, of 140 ± 10 ms, a mean rise time, defined as the time taken from 5 to 95% of the peak amplitudes of 190 ± 15 ms and a mean half-width, defined as the time the signals spends beyond 50% of the peak amplitude of 850 ± 40 ms (Fig. 2). Invariably the decaying phase of the IJP was interrupted by a rebound potential. We are unclear about the events underlying the rebound potential. Rebound potentials were unaffected by adding caesium ions (2 mM) or nickel ions (0.1 mM) ($n = 3$ for each agent) and were not triggered by periods of membrane hyperpolarization (see Fig. 3). The rebound potential

was invariably abolished when both components of the IJP were abolished: on occasions the rebound potential was abolished when the slow component was abolished (Fig. 2*E*) but this was not always the case (Fig. 2*H*). This phenomenon has not been examined further. In some preparations, the rebound potential was followed by a long-lasting depolarization which persisted after the IJP had been abolished (Fig. 2*D–F*). This slow potential appeared to result from the release of substance P from excitatory nerves; it was abolished by desensitizing the preparations with substance P (10 μM) for 20 min ($n = 3$; Niel *et al.* 1983*b*; Lyster *et al.* 1992).

The two components of the IJP could be separated by adding apamin or NOLA to the perfusion fluid (Fig. 2). The amplitude of IJPs was reduced by apamin (0.1 μM), the time to onset of the IJP was increased and the half-width of the IJP was increased (Fig. 2*A* and *B*). In solutions containing apamin, IJPs had a mean peak amplitude of 15.2 ± 1.1 mV ($n = 10$), a mean latency of 200 ± 35 ms, a mean rise time of 450 ± 20 ms and a mean half-width of 1130 ± 45 ms. The apamin-resistant component of the IJP was abolished by the further addition of NOLA (10 μM; Fig. 2*C*). When NOLA and apamin were applied in the reverse order, NOLA (10 μM) also reduced the amplitude of the IJP, the time to onset was little changed but the half-width of the IJP was shortened (Fig. 2*D* and *E*). In solutions containing NOLA, IJPs had a mean peak amplitude of 14.8 ± 1.8 mV ($n = 6$), a mean latency of 175 ± 15 ms, a mean rise time of 195 ± 10 ms and a mean half-width of 460 ± 30 ms.

The NOLA-resistant component of the IJP was abolished by the further addition of apamin (0.1 μM; $n = 5$; Fig. 2*F*). The NOLA-resistant component was also reduced in amplitude by PPADS, a blocker of purinergic receptors in the gut (Windscheif *et al.* 1995). At a concentration of 100 μM the amplitude of the NOLA-resistant component was reduced from a value of 16.8 ± 4.8 mV to 13.0 ± 4.1 mV; increasing the

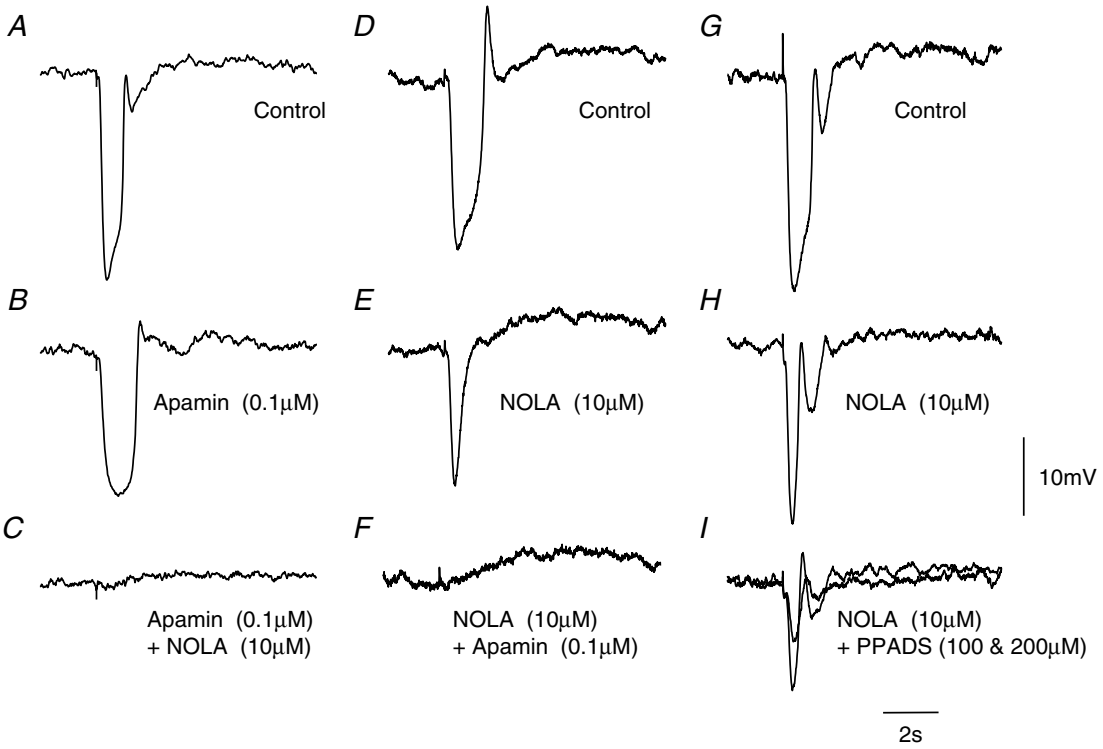

Figure 2. Effects of apamin, NOLA and PPADs on IJPs recorded from the circular layer of guinea-pig proximal colon

The left-hand column of traces shows a control IJP evoked by supramaximal nerve stimulation (*A*), the response recorded in apamin (*B*), and in apamin applied together with NOLA (*C*). The resting membrane potential was −46 mV throughout. The central column of traces shows a control IJP (*D*), the response recorded in NOLA (*E*), and in NOLA applied together with apamin (*F*). The resting membrane potential was −44 mV throughout. The right-hand column of traces shows a control IJP (*G*), the response recorded in NOLA (*H*), and in NOLA applied together with two different concentrations of PPADS (*I*), with the smaller response being detected in the higher concentration of PPADS. The resting membrane potential was −47 mV throughout. The time and voltage calibration bars apply to all recordings. Atropine (1 μM) and nifedipine (1 μM) were present throughout.

concentration of PPADS to 200 μM further reduced the amplitude to 6.9 ± 2.3 mV ($n = 4$). The effects of NOLA were not reversed by washing the preparations with drug-free solution for up to 3 h. On the other hand the effects of apamin were completely reversed by washing with drug-free solutions for 1–1.5 h. In several experiments, attempts were made to separate the two components of the IJP by varying the stimulus strength, this was never successful. Thus whatever stimulus strength was applied, a part of the biphasic response was removed by the addition of apamin to the physiological saline. Clearly if the two components result from transmitter release from two separate populations of nerve fibres, the two sets of fibres have very similar thresholds for excitation. The apamin-resistant component was unaffected by IbTX (0.1 μM; $n = 3$), 9-AC (1 mM; $n = 3$), NFA (100 μM; $n = 3$), or glibenclamide (10 μM; $n = 3$).

When intracellular recordings were made from electrically short strips of circular muscle dissected from the proximal colon, cells were found to have resting potentials in the range −37 to −47 mV (−44.0 ± 0.8 mV, $n = 17$). The recordings showed evidence of an ongoing discharge of membrane noise (Fig. 3*B* and *C*) whose spectral density curves could be described as for recordings from other regions of the gut (Edwards *et al.* 1999). Single supra-maximal stimuli evoked IJPs with similar characteristics to those recorded from sheets of tissue. When impaled with two independent electrodes, one being used to pass current and the other to record membrane potential changes, hyperpolarizing current pulses evoked electrotonic potentials whose time courses of onset, or offset, could be described with single exponentials having time constants in the range 70–300 ms (160 ± 20 ms, $n = 14$). Preparations had input resistances in the range

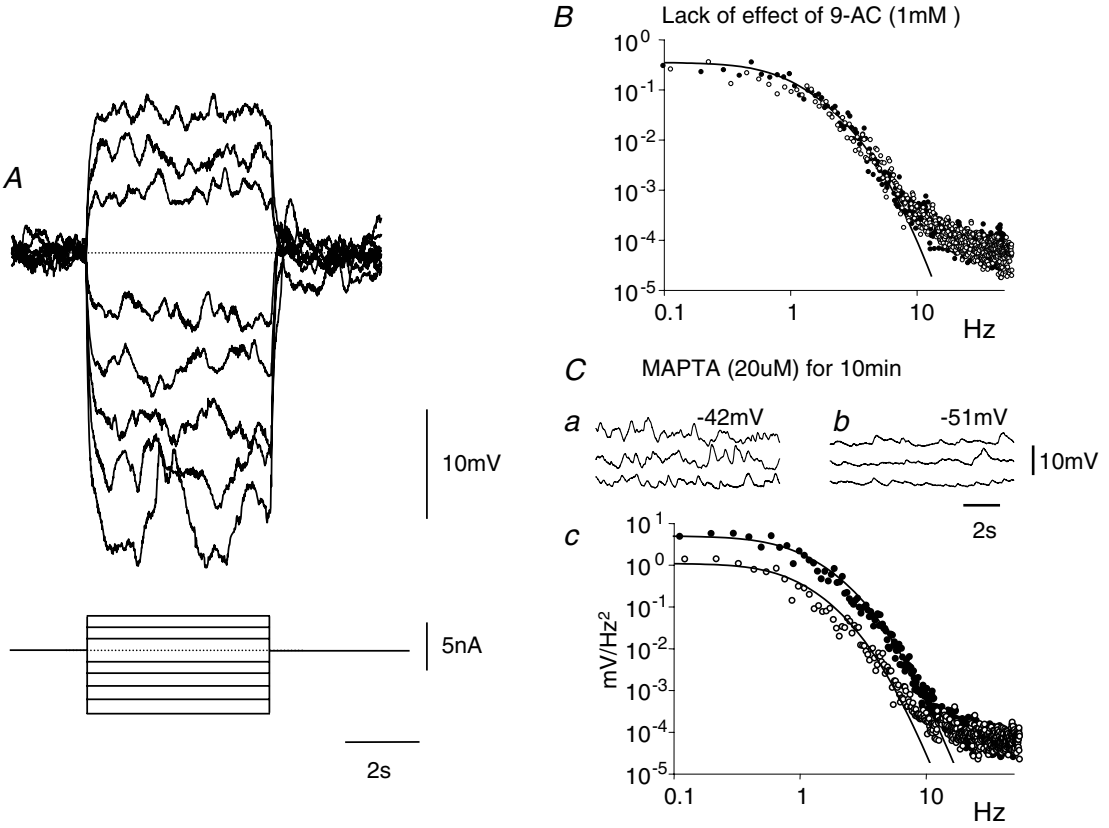

Figure 3. Electrical properties of muscle bundle from the circular layer of guinea-pig distal colon
A, the effects of injecting a series of hyperpolarizing and depolarizing currents on the membrane potential of a short bundle of muscle isolated from the distal colon. Note that the discharge of membrane noise was little affected throughout. The resting potential of this preparation was −44 mV; the time current and voltage calibration bars apply to recordings shown in *A*. *B,* spectral density curves illustrating that the discharge of membrane noise (●) was unaffected by adding 9-AC (○) to the physiological saline; the resting potential of the preparation remained unchanged at −40 mV throughout. *C*, the discharge of membrane noise (●) was reduced by adding MAPTA-AM (20 μM; ○) to the physiological saline for 10 min (*Cc*). Note that the reduction in membrane noise was associated with an increase in resting potential from −42 mV (*Ca*) to −51 mV (*Cb*). Atropine 1 μM and nifedipine (1 μM) were present in each experiment.

2.0–9.9 MΩ (4.9 ± 0.7 MΩ, $n = 14$). In each of the preparations tested, hyperpolarizing or depolarizing current pulses failed to evoke a regenerative response either during the periods of depolarization or after the break of periods of hyperpolarization (Fig. 3*A*). Moreover, unlike the antrum (Teramoto & Hirst, 2003), the discharge of membrane noise was not abolished by periods of hyperpolarization (Fig. 3*A*). Again, unlike the antrum, the discharge of membrane noise was unaffected by 9AC (1 mM; $n = 3$; Fig. 3*B*) or by NFA (200 μM; $n = 3$). However like the antrum, the discharge of membrane noise was reduced so that individual unitary potentials could be detected by adding MAPTA (20 μM) to the physiological saline for a period of 10 min: at the same time the amplitude of the power spectral density curve was reduced (Fig. 3*C*). This was associated with a membrane hyperpolarization, in the range 2−11 mV (7.1 ± 1.6 mV, $n = 5$).

Properties of IJPs recorded from the circular layer of guinea-pig proximal colon

That the IJP was made up of two separate components could also be demonstrated by adding ODQ (3 μM), an inhibitor of soluble guanylate cyclase, to the physiological saline. ODQ, like NOLA reduced the amplitude of the apamin-resistant component (Fig. 4*A–C*). When ODQ (3 μM) was applied before apamin the rapid component persisted and this was in turn blocked by apamin (0.1 μM; Fig. 4*D–F*). In these experiments, the ODQ-resistant component had a mean peak amplitude of 18.0 ± 1.4 mV ($n = 8$), a mean latency of 160 ± 10 ms, a mean rise time of 160 ± 5 ms and a mean half-width of 370 ± 15 ms.

In the presence of apamin (0.1 μM) and ODQ (3 μM) nerve stimulation evoked an IJP with a peak amplitude of 1.0 ± 0.4 mV ($n = 5$). The inhibitory effect of ODQ, like that of apamin, was reversed by washing with drug-free solution for 1–1.5 h.

Clearly the two components of the IJP could result if two transmitters, presumably ATP and NO (Watson *et al.* 1996) were released by intrinsic inhibitory nerve terminals and activated two distinct sets of potassium-selective channels. For this to be the case ATP must activate an apamin-sensitive K^+ channel and NO must activate a novel potassium-selective channel that is insensitive to both IbTX and glibenclamide. Alternatively, ATP could activate apamin-sensitive K^+ channels and NO could

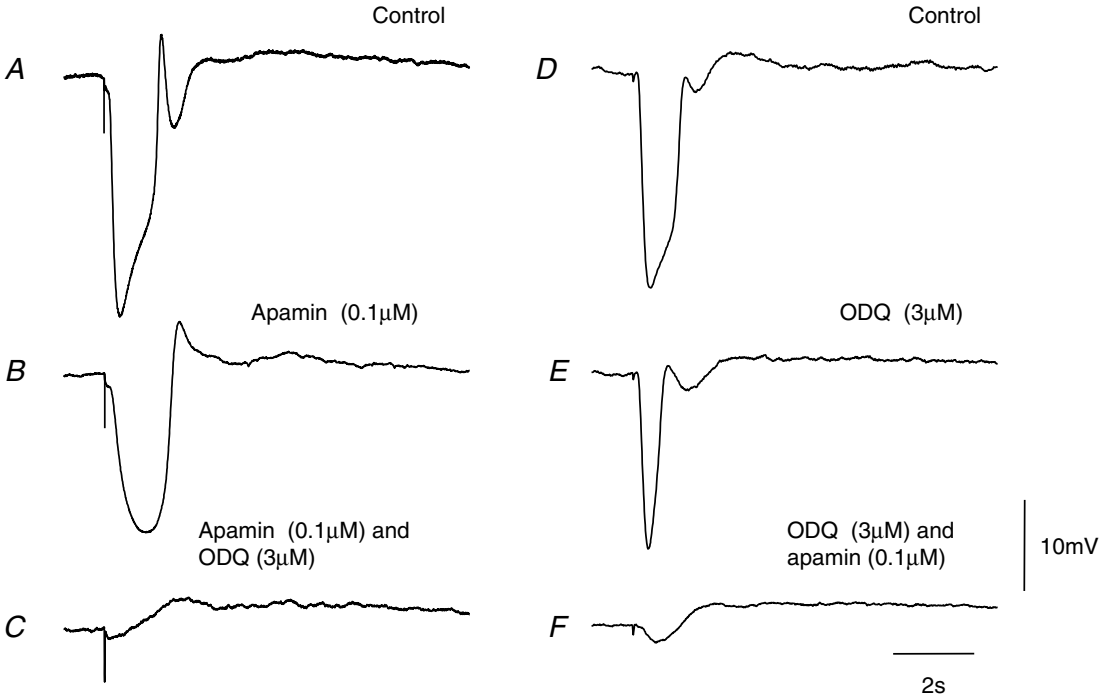

Figure 4. Effect of apamin and ODQ on IJPs recorded from the circular layer of guinea-pig proximal colon

The left-hand column of traces shows a control IJP evoked by supramaximal nerve stimulation (*A*), the response recorded in apamin (*B*), and in apamin applied together with ODQ (*C*). The resting membrane potential was −48 mV throughout. The right-hand column of traces shows a control IJP (*D*), the response recorded in ODQ (*E*), and in ODQ applied together with apamin (*F*). The resting membrane potential was −45 mV throughout. The time and voltage calibration bars apply to all recordings; each trace is an average of 20 successive recordings. Atropine (1 μM) and nifedipine (1 μM) were present throughout.

produce a hyperpolarization by decreasing a resting inward current. Attempts were made to distinguish between these two possibilities by calculation (see Methods and Fig. 1*A*). Firstly the rapid component was attributed to a brief increase in g_K and the second component was attributed to a slower-in-onset longer-lasting increase in g_K (Fig. 5*B*). When the conductances, adjusted so that they had similar time courses and amplitudes to those of the separate components recorded experimentally, were summed, an IJP resembling that recorded from intact tissues was generated (Fig. 5*A* and *B*). In the second simulation, the rapid component was attributed to a brief increase in g_K and the second component was attributed to a slower-in-onset longer-lasting decrease in g_{Na} (Fig. 1*A*). Again when these two distinct conductance changes were summed together, an IJP resembling that recorded from intact tissues was generated (Fig. 5*A* and *C*). Clearly these simple simulations were unable to cast further light on the nature of the conductance changes underlying the biphasic IJP. All of the subsequent experiments were designed to test whether both components of the IJP resulted from an increase in g_K, or whether the nitrergic component resulted from a decreased inward current.

Effect of changing $[K^+]_o$ on IJPs recorded from the circular layer of guinea-pig proximal colon

In the first series of experiments the effect of changing the external concentration of potassium ions, $[K^+]_o$, without osmotic compensation, on the amplitudes of the two components was examined. In each experiment, the preparation was bathed in a solution containing apamin (0.1 μM) and the effect of changing $[K^+]_o$ (from 5 to

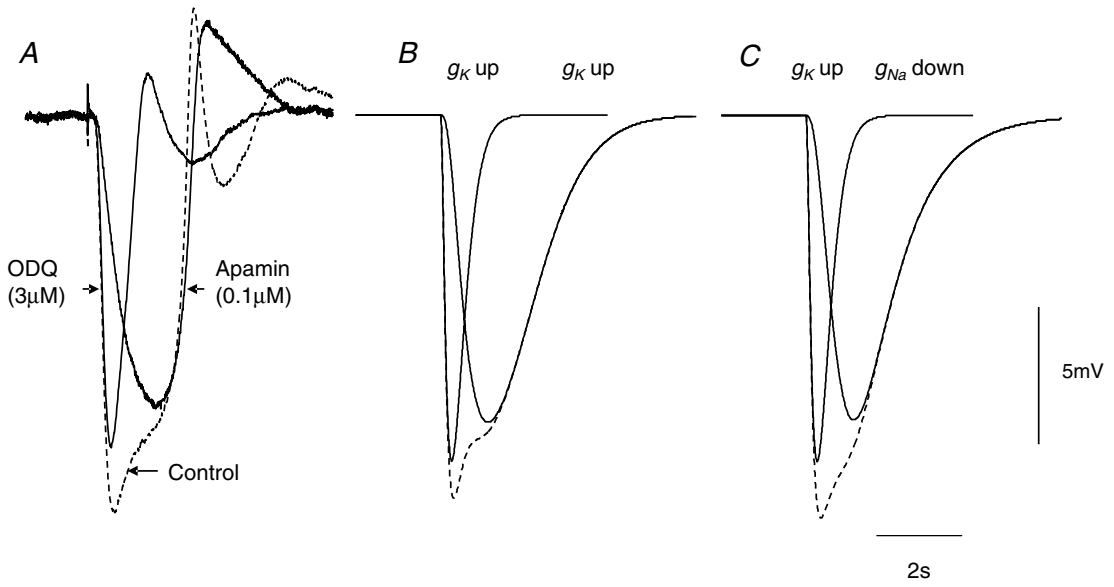

Figure 5. Comparison between experimental determinations of time courses of colonic IJPs with simulations of colonic IJPs

The three overlaid traces presented in *A* show a control response (dashed line) and responses recorded in either apamin or ODQ; all recordings made from the same cell, resting membrane potential was −48 mV throughout. The three overlaid traces in *B* show calculated IJPs in which the both the rapid and slow components of the IJP were assumed to be generated by a brief and a slower increase in g_K; the response to the sum of these conductance changes is shown as a dashed line. The time course of the initial rapid modulation was defined, using eqn (1) (Methods) as the difference between two exponential functions, raised to a power, *N*, where *g* represented the modulation in g_K, *M* scaled the peak modulation to 14 nS, *A* and *B* took values of 0.2 s and 0.1 s, respectively, and the exponent *N* was 1. For the secondary slower modulation the same approach was taken using a value of 100 nS for *M*, with *A* and *B* taking values of 0.9 s and 0.85 s and *N* taking a value of 1.6. The three traces in *C* show calculated IJPs in which the rapid component of the IJP was assumed to be generated by a brief increase in g_K, using the values of constants given above, followed by the slow component which was assumed to be generated by a decrease in g_{Na} using eqn (1) (Methods): *M* was chosen to give a 98% peak reduction in g_{Na}, with *A* and *B* taking values of 1 s and 0.95 s, respectively, and *N* taking a value of 2. The response to the sum of these conductance changes is shown as a dashed line. The time and voltage calibration bars apply to all recordings of membrane potential and each set of simulations. Atropine (1 μM) and nifedipine (1 μM) were present in recordings shown in *A*; each experimental trace is an average of 20 successive recordings.

2.5 mM and from 5 to 10 mM) on the amplitudes of the nitrergic component of the IJP was determined. Subsequently the preparations were washed with drug-free solution for 1.5 h and ODQ (0.3 μM) was then added to the bathing medium. The effect of changing $[K^+]_o$ on the amplitudes of the purinergic component of the IJP was then determined. These changes in $[K^+]_o$ had little effect on the resting membrane potential of the preparations, with the membrane potential being -39.5 ± 1.0, -42.7 ± 1.0 and -38.5 ± 0.9 mV when $[K^+]_o$ was 2.5, 5 and 10 mM, respectively ($n = 5$). The results of one experiment are illustrated in Fig. 6*A* and *C*. It can be seen that the amplitude of the nitrergic component of the IJP, recorded in apamin, was little changed by changing $[K^+]_o$ in the range 2.5–10 mM (Fig. 6*A*): the results from this experiment and four experiments are shown graphically in Fig. 6*B*. In contrast the amplitude of the purinergic component of the IJP, recorded in ODQ, increased when $[K^+]_o$ was decreased and decreased when $[K^+]_o$ was increased (Fig. 6*C*): the grouped results are plotted in Fig. 6*D*. Statistical analysis showed that the slope of the relationship between the amplitudes of the purinergic IJPs and $[K^+]_o$ was negative, -5.2 ± 1.0 mV $(pK)^{-1}$, and significantly different to zero ($P < 0.01$): this was not the case for the relationship between nitrergic IJPs and $[K^+]_o$.

These observations suggest that the purinergic component of the IJP involves an increase in g_K and that a similar but slower increase in g_K does not contribute to the nitrergic component of the IJP.

Effect of changing membrane potential on IJPs recorded from the circular layer of guinea-pig proximal colon

The effect of changing the membrane potential of bundles of circular muscle on the amplitude of the nitrergic component of the IJP was explored in two ways. Firstly two simulations were constructed which would predict the behaviour of nitrergic IJPs if they resulted from an increase in g_K or if they resulted from a suppression of the discharge of membrane noise (see Methods and

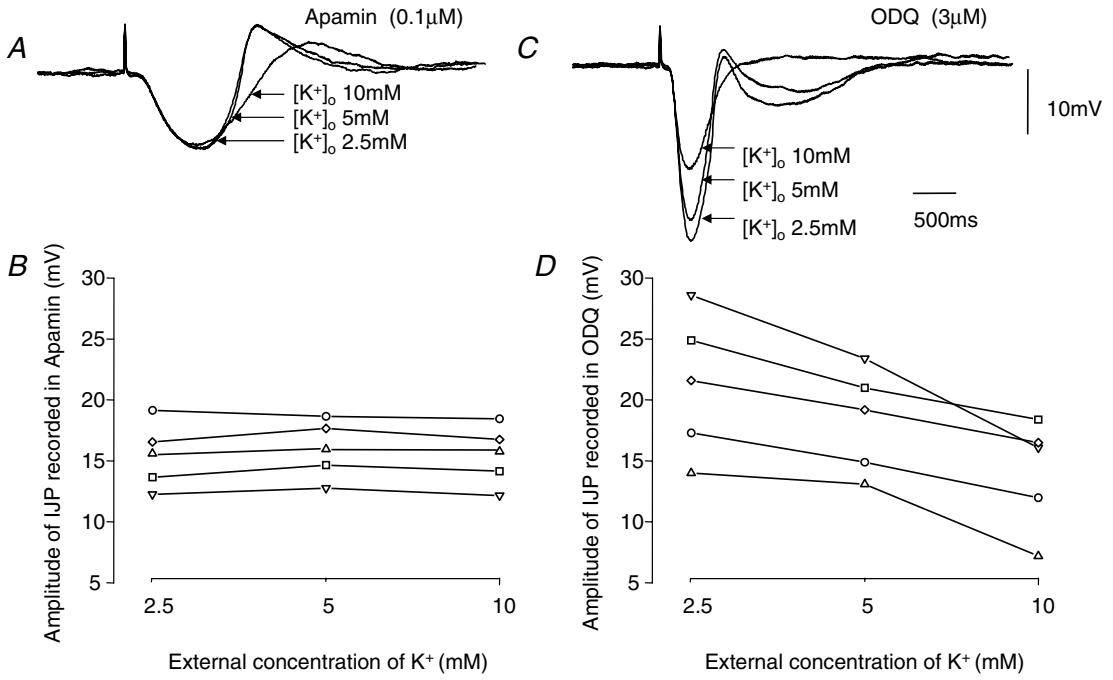

Figure 6. Effect of changing $[K^+]_o$ on amplitudes of nitrergic and purinergic compoents of IJP recorded from the circular layer of guinea-pig proximal colon

The three overlaid traces in *A* show the effect of changing $[K^+]_o$ from 2.5 to 5 to 10 mM on the amplitudes of the nitrergic component of the IJP, recorded in the presence of apamin. The resting potential in 2.5 and 5 mM $[K^+]_o$ was −40 mV; it fell to −34 mV in 10 mM $[K^+]_o$. *B* shows the results from this and four other experiments plotted graphically. The three overlaid traces in *C* show the effect of changing $[K^+]_o$ from 2.5 to 5 to 10 mM on the amplitudes of the purinergic component of the IJP, recorded from the same cell in the presence of ODQ. *D* shows the results from this and four other experiments plotted graphically. The time and voltage calibration bars apply to all recordings of membrane potential, each trace is the average of 5 successive recordings. Atropine (1 μM) and a nifedipine (1 μM) were present throughout.

Fig. 1*B*). As expected the amplitudes of computed IJPs decreased as the membrane potential was made more negative when they were assumed to result from an increase in g_K (Fig. 7*A*): when nitrergic IJPs were simulated by assuming that they resulted from a suppression of the discharge of membrane noise, they increased in amplitude as the membrane potential was made more negative (Fig. 7*B*). Secondly the effect of changing the membrane potential on the amplitude of nitrergic IJPs was determined experimentally by impaling a segment with two independent electrodes, one being used to pass current and the other to record membrane potential changes: in these experiments preparations were bathed in solutions containing apamin (0.1 μM) to abolish the purinergic component of the IJP. When this was done, the amplitude of the nitrergic IJP increased as the membrane potential was made more negative (Fig. 7*C* and *D*). Over the limited range of membrane potentials examined, the relationship between peak amplitude of the nitrergic IJP was well described by a straight line with, in the experiment shown in Fig. 7, an extrapolated reversal potential of +35 mV (Fig. 7*D*). From this and the other experiments in this series the mean reversal potential obtained by extrapolation was $+12.5 \pm 5.6$ mV ($n = 6$). These experiments suggest that the nitrergic component of the IJP results from a reduction in inward current flow rather than from an increased outward flow of K^+.

In the second series of experiments the effects of changing membrane potential on the time course of two component IJPs were examined. Again simulations were constructed and the results of the simulations were compared with physiological measurements. In the two

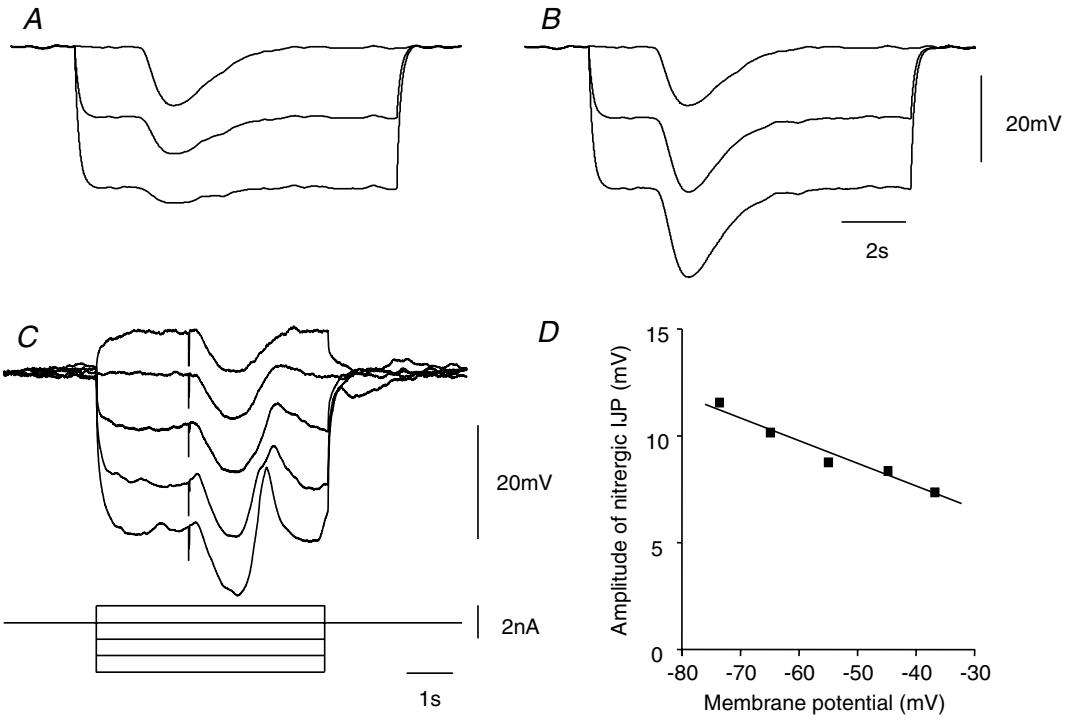

Figure 7. Effect of changing membrane potential on nitrergic IJPs recorded from the circular layer of guinea-pig proximal colon

The upper two sets of traces illustrate calculations which show the effect of changing the membrane potential on the nitrergic component of the IJP if it was assumed to result from an increase in g_K (*A*) or if it was assumed to result from a decrease in g_{cation} (*B*): each of these traces shows the average of 40 calculations. For details of calculations see Methods. Note that if the IJP resulted from an increase in g_K, the amplitude of the IJP decreased as the membrane potential approached the potassium reversal potential (E_K). Conversely if the IJP resulted from a decrease in g_{cation}, the amplitude of the IJP increased as the membrane potential approached E_K. The upper time and voltage calibration bars apply to both sets of simulations. The overlaid traces in *C* show the effects of changing membrane potential on the nitrergic component of the IJP; these results are plotted graphically in *D* and show that the amplitude of the IJP increases with membrane hyperpolarization. The lower time, voltage and current calibration bars apply to experimental observations; each experimental trace is the average of 4 successive responses and the resting potential was −44 mV. Apamin (0.1 μM) atropine (1 μM) and nifedipine (1 μM) were present throughout.

simulations shown in Fig. 8 the biphasic IJP was assumed to result from two kinetically distinct increases in g_K (Fig. 8*A*) and from an initial increase in g_K augmented by a slower suppression of the discharge of membrane noise (Fig. 8*B*). When the effect of changing the membrane potential on simulated IJPs resulting from two separate increases in g_K was examined, the amplitudes of both components were found to be reduced with no overall change in the shape, hence the time to peak amplitude of the IJP was unchanged (Fig. 8*A*). In contrast when the simulated IJPs resulted from an increase in g_K and a suppression of membrane noise, hyperpolarization increased the time to peak of the simulated IJP as the contribution made by the initial increase in g_K reduced and that made by slower suppression of inward current increased (Fig. 8*B*). When the effect of changing the membrane potential on the two-component IJP was determined experimentally the time to peak of the composite IJP was found to increase as the membrane potential was made more negative (Fig. 8*C*). In the experiment illustrated, hyperpolarizing the membrane from −47 to −77 mV increased the time to peak from 450 to 820 ms. From this and the other experiments in this series the mean time to peak was found to increase from 455 ± 25 to 650 ± 50 ms ($n = 6$) with a hyperpolarizing step of approximately 30 mV; these values

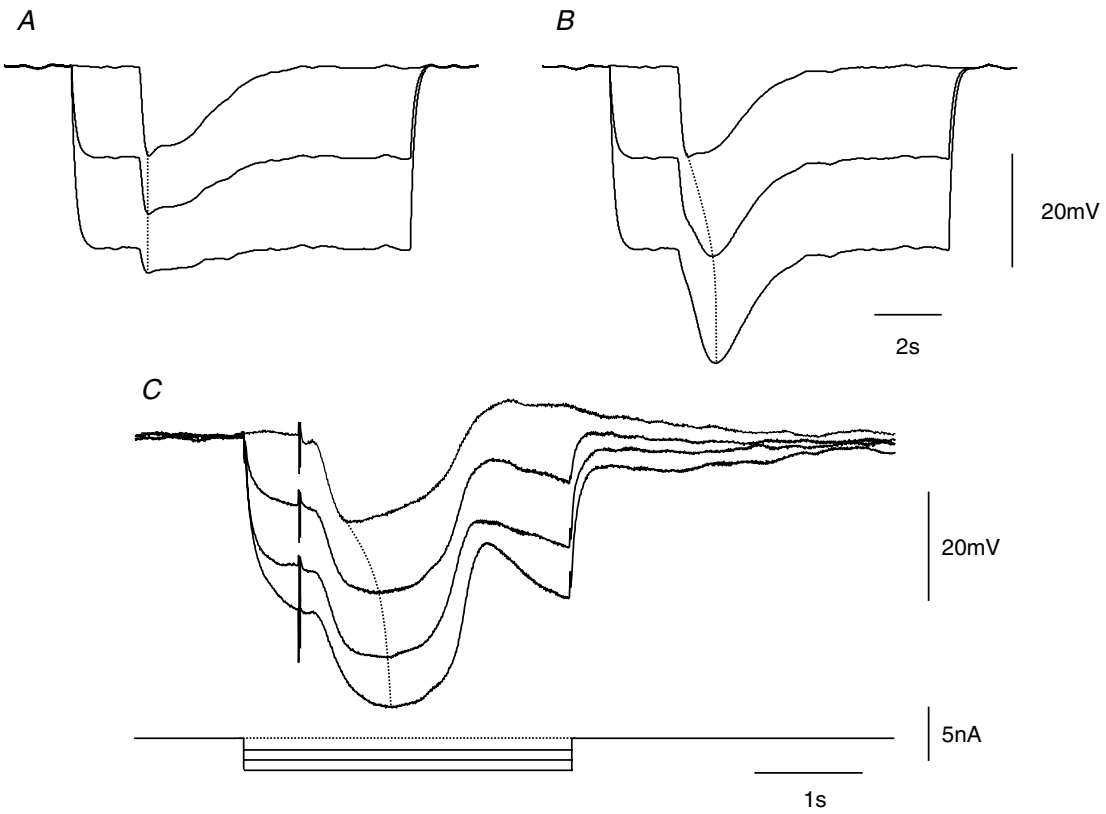

Figure 8. Effect of changing membrane potential on composite IJPs recorded from the circular layer of guinea-pig proximal colon

The upper two sets of traces illustrate calculations which show the effect of changing the membrane potential on the control IJP if it was assumed to result from a brief followed by a slower increase in g_K (*A*) or if it was assumed to result from a brief increase in g_K followed by a decrease in g_{cation} (*B*). For details of calculations see Methods. Note that if the IJP resulted from two separate increases in g_K, the time course the IJP did not change as the membrane potential approached E_K, with the time to peak hyperpolarization, shown by a dotted line, remaining constant. Conversely if the IJP resulted from an initial increase in g_K followed by a decrease in g_{cation}, the time to peak of the IJP, shown by dotted line, increased as the membrane potential approached E_K. The upper time and voltage calibration bars apply to both sets of simulations. The overlaid traces in *C* show the effects of changing membrane potential on the control IJP. Note that the time to peak hyperpolarization, again shown by a dotted line, increased as the membrane potential was made more negative. The lower time, voltage and current calibration bars apply to experimental observations; each experimental trace is the average of 4 successive responses whereas the computations illustrate the average of 40 successive computations. Atropine (1 μM) and nifedipine (1 μM) were present throughout.

were significantly different using a paired t test. These experiments support the idea that the purinergic and nitrergic components of the IJP result from two quite distinct changes in membrane conductance.

When recordings were made from isolated bundles of the circular layer of the proximal colon, as pointed out previously, a discharge of membrane noise was apparent. In these preparations when the nitrergic component of the IJP was inspected, it appeared to be associated with a cessation of the discharge of membrane noise (Fig. 9*E*). To test this idea, the standard deviation time course was determined for baseline recordings, during the nitrergic IJP and during the rebound depolarization. When this was done, the standard deviation fell during the nitrergic component of the IJP and increased during the rebound depolarization (Fig. 9*G*). The mean fall in the standard deviation, determined at the average peak of the nitrergic IJP (Fig. 9*F*) was 1.05 ± 0.3 mV ($n = 5$).

A fall in standard deviation during the nitrergic IJP may result from a conductance increase which had shorted out the discharge of membrane noise or if the discharge of membrane noise had been interrupted, and attempts were therefore made to distinguish between these two possibilities using a mathematical simulation. Again the nitrergic IJP was presumed to result either from an increase in g_K (Fig. 9*A*) or from a suppression of the discharge of membrane noise (Fig. 9*C*). In the simulation when an increase in g_K was applied, no change in the standard deviation of the membrane noise was detected (Fig. 9*B*). This implies that as the membrane noise is shorted out by the increase in membrane conductance, the associated hyperpolarization increases the amplitude of the membrane noise by increasing its driving potential. Conversely when the IJP was calculated to arise from a suppression of noise discharge, the standard deviation of the membrane noise fell dramatically (Fig. 9*D*). Together

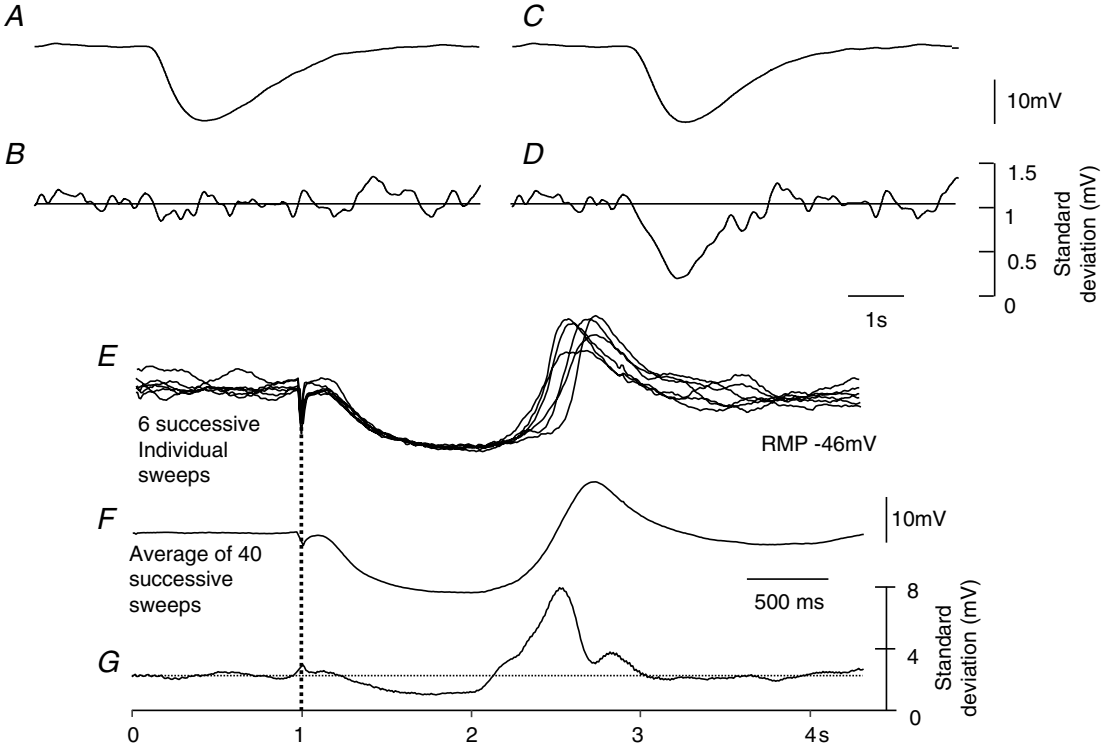

Figure 9. Change in standard deviation of membrane noise during a nitrergic IJP recorded from the circular layer of guinea-pig proximal colon

The upper two sets of traces illustrate calculations which show the effect of the nitrergic component of the IJP on the standard deviation if it was assumed to result from an increase in g_K (*A* and *B*) or if it was assumed to result from a decrease in the discharge of unitary potentials by ICC_{IM} (*C* and *D*). For details of calculations see Methods. Note that if the IJP resulted from an increase in g_K, the standard deviation was unchanged during the IJP. Conversely if the IJP resulted from a decrease in the discharge of unitary potentials by ICC_{IM}, the standard deviation fell during the IJP. The overlaid experimental traces shown in panel *E* show 6 successive responses to nerve stimulation; the average of 40 successive sweeps is shown in *F*. When the mean standard deviation for the successive 40 traces was calculated (*G*), it was found that the standard deviation fell during the IJP and increased during the rebound potential. The lower time, and current calibration bars apply to experimental observations. Apamin (0.1 μM) atropine (1 μM) and nifedipine (1 μM) were present throughout.

these observations indicate that the depression in standard deviation detected during the nitrergic component of the IJP is unlikely to result from an increase in g_K.

Discussion

These experiments have shown that inhibitory nerve stimulation evokes a two-component IJP in the circular layer of the proximal guinea-pig colon. The initial component of the IJP results, at least in part, from the release of ATP and the subsequent activation of apamin-sensitive K^+-selective channels. In contrast the second component of the IJP results from the concurrent release of NO and the subsequent suppression of an ongoing inward current via a pathway involving the formation of cyclic GMP. Presumably the ongoing discharge of membrane noise results from the discharge of unitary potentials by colonic ICC_{IM} and neurally released NO inhibits this discharge.

Control recordings from short segments of colonic circular muscle detected an ongoing discharge of membrane noise with a characteristic frequency spectrum (Fig. 3*B* and *C*). Such spectral density curves have been obtained from the circular layer of other regions of the gastrointestinal tract but only when the preparations contain ICC_{IM}. Thus a discharge of membrane noise is detected in the antral circular layer of control animals but not in tissues taken from W/W^V mice which lack ICC_{IM} (Dickens *et al.* 2001; Beckett *et al.* 2004). Similarly discharges of membrane noise are detected in fundal tissues which contain ICC_{IM} but are absent in both W/W^V and Sl/Sl^d mice, each of which lack ICC_{IM} (Beckett *et al.* 2002). On this basis it seems likely that the discharge of noise detected in the colon results from ongoing activity generated by colonic ICC_{IM}. Unlike antral ICC_{IM}, the frequency of discharge of fundal ICC_{IM} is little affected by changes in membrane potential, suggesting that fundal ICC_{IM} either lack a voltage sensor or the cells are held at a membrane potential that is well away from their voltage-sensitive range (Beckett *et al.* 2004). The same also appears to apply to colonic ICC_{IM}. Regenerative responses, like those detected in antral tissue were not triggered by membrane depolarization or by the releasing the ICC_{IM} from hyperpolarized levels (Fig. 3*A*). Furthermore, unlike the antrum, periods of hyperpolarization failed to inhibit the discharge of membrane noise (Fig. 3*A*; Teramoto & Hirst, 2003). Similarly, unlike the antrum (Hirst *et al.* 2002*b*), but like the fundus (Beckett *et al.* 2004), the application of chloride channel blockers failed to block the discharge of membrane noise. Together these observations support the view that ICC_{IM} in different regions of the gut may have quite distinct properties with colonic ICC_{IM} appearing to resemble more closely those found in the fundus (Beckett *et al.* 2004).

Virtually all IJPs recorded from many different regions of the gut consist of two components, an initial purinergic, apamin-sensitive component, followed by a nitrergic, apamin-insensitive, component (Niel *et al.* 1983*a*; Lyster *et al.* 1992; He & Goyal, 1993; Teramoto & Hirst, 2003). When tested the nitrergic component has been found to be abolished by ODQ, an inhibitor of soluble guanidine cyclase (Ward *et al.* 1992; Teramoto & Hirst, 2003), suggesting that neurally released NO causes the formation of cyclic GMP in target cells.

When the role of ICC_{IM} in inhibitory neurotransmission has been examined, it has been found that the nitrergic component is absent in tissues devoid of ICC_{IM} (Burns *et al.* 1996; Beckett *et al.* 2002; Suzuki *et al.* 2003), suggesting that neurally released NO selectively targets ICC_{IM}. In the antrum, neurally released NO reduces the ongoing discharge of unitary potentials by ICC_{IM} and this results in a small hyperpolarization (Teramoto & Hirst, 2003). In the colon nitrergic nerve stimulation also causes a fall in discharge of membrane noise and this is reflected as a fall in the standard deviation of the membrane potential recordings (Fig. 9). However the nitrergic component of inhibitory responses in the colon is of much larger amplitude than those of the antrum. One explanation for this could simply be that colonic ICC_{IM} produce a larger mean inward current than do those of the antrum. Some support for this suggestion comes from the finding that in the antrum, when the discharge of membrane noise is blocked by buffering $[Ca^{2+}]_i$ to low levels a small depolarization is detected (Fukuta *et al.* 2002). This presumably reflects the balance between the suppression of inward current, generated by antral ICC_{IM}, and the suppression of Ca^{2+}-dependent outward currents, generated either by ICC_{IM} or smooth muscle cells. In the colon, buffering $[Ca^{2+}]_i$, to low levels produce a hyperpolarization of some 7 mV (Fig. 3*C*). An increased contribution of inward current flow by colonic ICC_{IM} could result from the conductance change they generate having a more positive reversal potential than that of antral ICC_{IM}. Alternatively the density of colonic ICC_{IM} could be higher or their rates of discharge of unitary potentials could be greater than those of antral ICC_{IM}.

In the antrum unitary potentials involve ion channels which are blocked by chloride channel antagonists; when unitary potentials are abolished by such agents nitrergic IPJs are also abolished (Teramoto & Hirst, 2003). In the colon the discharge of membrane noise, by ICC_{IM}, is little affected by chloride channel blockers and the nitrergic component is similarly unaffected. In the antrum

hyperpolarization abolishes the resting discharge of membrane noise by ICC_{IM} and at the same time abolishes the nitrergic component of the IJP (Teramoto & Hirst, 2003). In the colon the resting discharge of membrane noise was little changed by membrane hyperpolarization (Fig. 3) and the amplitude of the nitrergic component was increased (Fig. 7). An increase in amplitude of a hyperpolarizing synaptic potential with increased membrane polarization can most simply be explained if the hyperpolarizing potential was initiated by a decrease in conductance to an ongoing inward conductance. Whilst such a phenomenon has been described in neuronal tissues (Weight & Padjen, 1973) and in cardiac cells (Bywater *et al.* 1990), a similar voltage dependency of IJPs has not been demonstrated in smooth muscle preparations. This type of behaviour is, however, implicit in the suggestion that in some regions of the gut nitrergic IJPs result from a suppression of chloride conductance (Crist *et al.* 1991*a*,*b*; Teramoto & Hirst, 2003). In the colon the extrapolated reversal potential for the IJP was some +12.5 mV. It would be unwise to assume that this reflected the reversal potential of the conductance being inhibited by neurally released NO. Quite clearly although this will represent the functional slope conductance change for the nitrergic component of the IJP at potentials near rest, any non-linearity in the conductance/membrane potential relationship will give a different absolute reversal potential. Furthermore, it is an implicit assumption that during the experiments described here, the preparations were isopotential. If this were not the case, even without non-linearities, the extrapolated reversal potential would be in error. Having made this point, however, it is clear that current polarization did effectively change the membrane potential of the preparations under test. If this were not the case, it is difficult to see how the nitrergic IJP would increase in amplitude when the membrane was hyperpolarized (Fig. 7) and it is difficult to understand how the time course of the composite IJP would change in the expected manner with hyperpolarization (Fig. 8).

In summary, the simplest explanation for our findings is that in the colon inhibitory nerve stimulation releases two separate transmitters, ATP which activates an apamin-sensitive potassium conductance and NO which selectively targets colonic ICC_{IM} and inhibits their resting discharge of unitary potentials. The two components can be distinguished on pharmacological grounds and on a kinetic basis with the slower nitrergic component involving the formation of a second messenger, cyclic GMP. The two components can be further distinguished on the basis of their ion selectivity in that the purinergic component involves an increase in g_K whereas the nitrergic involves a decreased inflow of depolarizing current, presumably by inhibiting the discharge of unitary potentials by colonic ICC_{IM}.

References

Baylor DA & Hodgkin AL (1973). Detection and resolution of visual stimuli by turtle photoreceptors. *J Physiol* **234**, 163–198.

Beckett EAH, Bayguinov YR, Sanders KM, Ward SM & Hirst GDS (2004). Properties of unitary potentials generated by intramuscular interstitial cells of Cajal in the murine and guinea-pig gastric fundus. J Physiol Accepted for publication subject to suitable change.

Beckett EAH, Horiguchi K, Khoyi M, Sanders KM & Ward SM (2002). Loss of enteric motor neurotransmission in the gastric fundus of *Sl/Sl*^{d} mice. *J Physiol* **543**, 871–887.

Burns AJ, Lomax AE, Torihashi S, Sanders KM & Ward SM (1996). Interstitial cells of Cajal mediate inhibitory neurotransmission in the stomach. *Proc Nat Acad Sci* **93**, 12008–12013.

Bywater RAR, Campbell GD, Edwards FR & Hirst GDS (1990). Effects of vagal stimulation and applied acetylcholine on the arrested sinus venosus of the toad. *J Physiol* **425**, 1–27.

Casteels R (1969). Calculation of the membrane potential in smooth muscle cells of the guinea-pig's taenia coli by the Goldman equation. *J Physiol* **205**, 193–208.

Crist JR, He XD & Goyal RK (1991*a*). Chloride-mediated junction potentials in circular muscle of the guinea pig ileum. *Am J Physiol* **261**, G742–G751.

Crist JR, He XD & Goyal RK (1991*b*). Chloride-mediated inhibitory junction potentials in opossum esophageal circular smooth muscle. *Am J Physiol* **261**, G752–G762.

Dalziel HH, Thornbury KD, Ward SM & Sanders KM (1991). Involvement of nitric oxide synthetic pathway in inhibitory junction potentials in canine proximal colon. *Am J Physiol* **261**, G789–G792.

Dickens EJ, Edwards FR & Hirst GDS (2001). Selective knockout of intramuscular interstitial cells reveals their role in the generation of slow waves in mouse stomach. *J Physiol* **531**, 827–833.

Edwards FR, Hirst GDS & Suzuki H (1999). Unitary nature of regenerative potentials recorded from circular smooth muscle of guinea-pig antrum. *J Physiol* **519**, 235–250.

Edwards FR, Redman SJ & Walmsley B (1976). Non-quantal fluctuations and transmission failures in charge transfer at Ia synapses on spinal motoneurones. *J Physiol* **259**, 689–704.

Fukuta H, Kito Y & Suzuki H (2002). Spontaneous electrical activity and associated changes in calcium concentration in guinea-pig gastric smooth muscle. *J Physiol* **540**, 249–260.

He XD & Goyal RK (1993). Nitric oxide involvement in the peptide VIP-associated inhibitory junction potential in the guinea-pig ileum. *J Physiol* **461**, 485–499.

Hirst GDS, Bramich NJ, Teramoto N, Suzuki H & Edwards FR (2002*b*). Regenerative component of slow waves in the guinea pig gastric antrum involves a delayed increase in $[Ca^{2+}]_i$ and Cl^- channels. *J Physiol* **540**, 907–919.

Hirst GDS, Dickens EJ & Edwards FR (2002*c*). Pacemaker shift in the gastric antrum of guinea-pigs produced by excitatory vagal stimulation involves intramuscular interstitial cells. *J Physiol* **541**, 917–928.

Hirst GDS & Ward SM (2003). Interstitial cells: involvement in rhythmicity and neural control of gut smooth muscle. *J Physiol* **550**, 337–346.

Kito Y, Fukuta H, Yamamoto Y & Suzuki H (2002). Excitation of smooth muscles isolated from the guinea-pig gastric antrum in response to depolarization. *J Physiol* **543**, 155–167.

Lyster DJ, Bywater RAR, Taylor GS & Watson MJ (1992). Effects of a nitric oxide synthase inhibitor on non-cholinergic junction potentials in the circular muscle of the guinea pig ileum. *J Auto Nerv Sys* **41**, 187–196.

Niel JP, Bywater RAR & Taylor GS (1983*a*). Apamin-resistant post-stimulus hyperpolarization in the circular muscle of the guinea-pig ileum. *J Auto Nerv Sys* **9**, 565–569.

Niel JP, Bywater RAR & Taylor GS (1983*b*). Effect of substance P on non-cholinergic fast and slow post-stimulus depolarization in the guinea-pig ileum. *J Auton Nerv Sys* **9**, 573–584.

Suzuki H & Hirst GDS (1999). Regenerative potentials evoked in circular smooth muscle of the antral region of guinea-pig stomach. *J Physiol* **517**, 563–573.

Suzuki H, Takano H, Yamamoto Y, Komuro T, Saito M, Kato K & Mikoshiba K (2000). Properties of gastric smooth muscles obtained from mice which lack inositol trisphosphate receptor. *J Physiol* **525**, 105–111.

Suzuki H, Ward SM, Bayguinov YR, Edwards FR & Hirst GDS (2003). Involvement of intramuscular interstitial cells in nitrergic inhibition in the mouse gastric antrum. *J Physiol* **546**, 751–763.

Teramoto N & Hirst GDS (2003). Interaction between excitatory and inhibitory metabotropic pathways in the guinea-pig antrum. *J Physiol* **550**, 181–189.

Van Helden DF, Imtiaz MS, Nurgaliyeva K, Von der Weid P & Dosen PJ (2000). Role of calcium stores and membrane voltage in the generation of slow wave action potentials in guinea-pig gastric pylorus. *J Physiol* **524**, 245–265.

Wang XY, Sanders KM & Ward SM (2000). Relationship between interstitial cells of Cajal and enteric motor neurons in the murine proximal colon. *Cell Tiss Res* **302**, 331–342.

Ward SM, Beckett EA, Wang X, Baker F, Khoyi M & Sanders KM (2000). Interstitial cells of Cajal mediate cholinergic neurotransmission from enteric motor neurons. *J Neurosci* **20**, 1393–1403.

Ward SM, Dalziel HH, Bradley ME, Buxton IL, Keef K, Westfall DP & Sanders KM (1992). Involvement of cyclic GMP in non-adrenergic, non-cholinergic inhibitory neurotransmission in dog proximal colon. *Br J Pharmacol* **107**, 1075–1082.

Watson MJ, Lang RJ, Bywater RAR & Taylor GS (1996). Characterization of the membrane conductance changes underlying the apamin-resistant NANC inhibitory junction potential in the guinea-pig proximal and distal colon. *J Auton Nerv Sys* **60**, 31–42.

Weight FF & Padjen A (1973). Slow synaptic inhibition: evidence for synaptic inactivation of sodium conductance in sympathetic ganglion cells. *Brain Res* **55**, 219–224.

Windscheif U, Pfaff O, Ziganshin AU, Hoyle CH, Baumert HG, Mutschler E, Burnstock G & Lambrecht G (1995). Inhibitory action of PPADS on relaxant responses to adenine nucleotides or electrical field stimulation in guinea-pig taenia coli and rat duodenum. *Br J Pharmacol* **115**, 1509–1517.

Zhang Y & Patterson WG (2002). Role of Ca^{2+}-activated Cl^- channels and MLCK in slow IJP in opossum esophageal smooth muscle. *Am J Physiol* **283**, G104–G114.

Acknowledgements

This project was supported by a grant from the Australian NH & MRC. Dr N. Teramoto was supported by a grant from the Ministry of Education, Science, Sports and Culture of Japan.